

Semiclassical Simulation of Homogeneous Emitter Ensembles with Local Dissipation

L. Ruks¹

¹Basic Research Laboratories & NTT Research Center for Theoretical Quantum Information, NTT, Inc., 3-1 Morinosato Wakamiya, Atsugi, Kanagawa, 243-0198, Japan
(Dated: February 17, 2026)

Emitter ensembles constitute a fundamental component in quantum optical technologies, yet efficient and accurate simulation of large ensembles remains challenging. Here, we formulate a truncated Wigner approximation (TWA) for permutation-invariant emitter ensembles subject to local dissipation by sampling stochastic trajectories in an extended phase space encompassing the Bloch sphere. Benchmarks show that the TWA accurately captures dynamics, including nonclassical signatures, with the approximation improving with ensemble size. We demonstrate large-scale simulations of hundreds of interacting ensembles within the TWA to reveal emergent spatial coherence and selective directionality of cooperative emission in a pumped 1D chain, highlighting a practical path to studying extended light-matter systems. Our results expand the scope of scalable simulations of quantum emitter ensembles, establishing a bridge between microscopic models and emergent behavior.

Homogeneous ensembles of indistinguishable emitters play a fundamental role in understanding and engineering open quantum systems. In state-of-the-art experiments featuring atoms [1–4] and solid-state [5–9] emitters, collective interactions commonly coexist with local dissipation. While this dissipation must often be mitigated, the interplay with collective dynamics can enable novel dissipative phases of matter [10–14] and distinct device functionalities enhanced by cooperativity [15–18]. As experiments enter the mesoscopic regime, exact simulations [10, 19–24] of minimal, permutation-invariant models are typically constrained to modest system sizes. This limitation motivates more scalable approximations [25] such as cumulant expansions [26, 27], tensor networks [28, 29], and (discrete) phase-space methods [30–35]. However, obtaining quantitatively controlled predictions at larger system sizes remains challenging, calling for targeted approaches [36, 37].

Semiclassical phase-space methods [38, 39] provide a powerful route to approximate many-body quantum dynamics, notably through the truncated Wigner approximation (TWA) [40, 41]. In the TWA, quantum evolution is represented by an ensemble average of semiclassical trajectories. Initial quantum fluctuations enter through random sampling, and in open systems dissipation contributes stochastic evolution. In the semiclassical limit, the approximation improves systematically, with quantum corrections entering perturbatively [41]. While well-established for bosons [42–45] and for spin ensembles with purely collective dynamics [46–50], an analogous semiclassical description of local dissipation in permutation-invariant ensembles has remained limited.

Here, we develop a semiclassical framework for the dynamics of permutation-invariant emitter ensembles (Fig. 1). Building on a quantum-to-classical mapping for variable-length spins [51], we formulate a truncated Wigner approximation in which the entire ensemble is described using just four phase-space variables that extend the usual Bloch sphere description. The additional

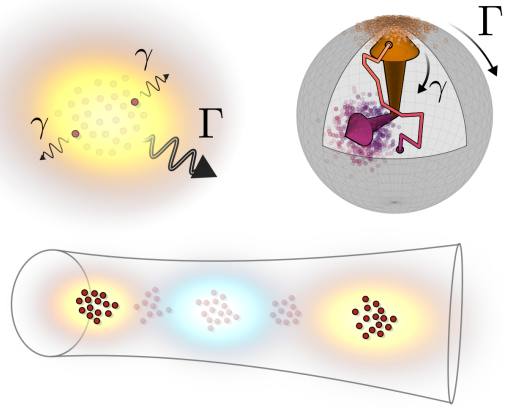


Fig. 1. (Bottom) An ensemble of emitters uniformly couples to a common field. (Top left) The ensemble emits collectively with rate Γ and undergoes independent local dissipation with rate γ . (Top right) In semiclassical simulations, the ensemble spin (large arrow) is sampled by classical phase-space variables (dots). Stochastic trajectories evolve along the Bloch sphere surface under collective processes, while local dissipation drives evolution into the sphere's interior.

variables capture changes in spin length induced by local dissipation, which enters through a few stochastic processes acting on semiclassical trajectories. In bad-cavity superradiance, and boundary time crystals, we find the method is accurate for small ensembles of tens of emitters—capturing squeezing and subradiance—and numerically approaches the exact solution for increasing ensemble size. The cost of the TWA scales only linearly with the number of distinct ensembles, enabling simulations corresponding to tens of thousands of emitters interacting through a resonator chain. In this extended nonlinear medium, we illustrate spatially structured dynamics under uniform pumping and a crossover to strong, selectively directional emission in response to a weak probe, highlighting a broad range of emergent cooperative phenomena in light-matter systems accessible with the TWA.

We consider a homogeneous ensemble formed from N two-level emitters indexed by n . Coupling to common modes induces coherent evolution under a Hamiltonian \hat{H} and collective dissipation via jumps \hat{L}^q built from collective spin operators $\hat{L}^0 = \hat{J}^z = \frac{1}{2} \sum_n \hat{\sigma}_n^z$, $\hat{L}^{\pm 1} = \hat{J}^{\pm} = \sum_n \hat{\sigma}_n^{\pm}$ where $\hat{\sigma}_n^0 \equiv \hat{\sigma}_n^z$, $\hat{\sigma}_n^{\pm 1} \equiv \hat{\sigma}_n^{\pm}$ are the Pauli- z and ladder operators of emitter n . Including statistically identical, independent dissipation, the system evolves under the Born-Markov master equation ($\hbar = 1$),

$$\dot{\hat{\rho}} = -i [\hat{H}, \hat{\rho}] + \sum_q \frac{\Gamma^q}{2} \mathcal{D} [\hat{L}^q] \hat{\rho} + \sum_{qn} \frac{\gamma^q}{2} \mathcal{D} [\hat{\sigma}_n^q] \hat{\rho}. \quad (1)$$

Here, $q = -1, 0, 1$ label decay, dephasing, and pumping, respectively, and $\mathcal{D}[\hat{X}]\hat{\rho} = 2\hat{X}\hat{\rho}\hat{X}^\dagger - \{\hat{X}^\dagger\hat{X}, \hat{\rho}\}$. Although phase-space descriptions of Eq. (1) have been established for $\gamma^q = 0$, a formulation valid more generally has remained limited.

To perform a semiclassical expansion of Eq. (1), we exploit invariance under permutation of emitters. Here, the ensemble dynamics can be equivalently expressed in the angular-momentum representation [20, 22, 52], where any permutation-invariant density matrix takes the form,

$$\hat{\rho} = \sum_{JMM'} \rho_{JMM'} |JM\rangle\langle JM'|. \quad (2)$$

In this representation, $|JM\rangle$ denotes collective kets labeled by eigenvalues $J(J+1)$ and M of total spin squared \hat{J}^2 and inversion \hat{J}^z respectively, and elements $|JM\rangle\langle JM'|$ are identified with the corresponding Dicke-state outer products in the full Hilbert space, averaged over permutation degeneracy [53]. The coefficients $\rho_{JMM'}$ then completely specify the state, with $\hat{\rho}$ block diagonal in J and collective operators acting purely as rotations in each block. Local decoherence induces population transfer between distinct sectors $J \leq N/2$ and, crucially, is expressed in the angular-momentum representation using only three effective jump operators [36] for each q :

$$\sum_n \mathcal{D} [\hat{\sigma}_n^q] \hat{\rho} = \sum_j \mathcal{D} [\hat{l}^{jq}] \hat{\rho}. \quad (3)$$

Acting on elements in Eq. (2), the jump operators \hat{l}^{jq} [53], for $j = -1, 0, 1$, couple both inversion $M \rightarrow M+q$ and total spin number $J \rightarrow J+j$ to neighboring sectors.

We establish the quantum-classical correspondence (details in [53]) for operators in Eq. (1) by applying a Stratonovich-Weyl (SW) mapping, developed for variable-spin systems [51, 54], in the representation Eq. (2). Each symmetric operator \hat{O} is assigned a Weyl symbol $\mathcal{O}(\mathcal{Z}) = \text{Tr}[\hat{O} \hat{\Delta}(\mathcal{Z})]$ and the density matrix is assigned a Wigner function $W(\mathcal{Z}) = \text{Tr}[\hat{\rho} \hat{\Delta}(\mathcal{Z})]$ of classical variables \mathcal{Z} . Expectations are then reproduced as averages, over W , of Weyl symbols. The kernel takes the

form [50, 55, 56] $\hat{\Delta}(\mathcal{Z}) = \hat{U}(\Omega) \hat{\Pi}_{\mathcal{J}} \hat{U}^\dagger(\Omega)$, for the collective rotation $\hat{U}(\Omega) = e^{-i\hat{J}_z\phi} e^{-i\hat{J}_y\theta} e^{-i\hat{J}_z\psi}$ by Euler angles $\Omega = (\phi, \theta, \psi)$. Here, rotations act on a parity operator $\hat{\Pi}_{\mathcal{J}}$ constructed to describe couplings between elements in Eq. (2) with distinct J . The Weyl symbol, $\mathcal{J}(\mathcal{J}+1)$, of \hat{J}^2 identifies the half-integer $\mathcal{J} = 0, 1/2, \dots$ as a classical total spin number analogous to J , while the conjugate angle ψ captures mixtures of spin lengths generated by local dissipation, seen by contrasting the Weyl symbols of local and collective jumps, \hat{l}^{jq} and \hat{L}^q :

$$\ell^{jq} = \chi_{jq}(\mathcal{J}) D_{qj}^{1*}(\phi, \theta, \psi), \quad \mathcal{L}^q = \chi_q(\mathcal{J}) D_{q0}^{1*}(\phi, \theta). \quad (4)$$

Here, D_{qj}^1 is the spin-1 Wigner- D matrix and χ_{jq}, χ_q are jump amplitudes [53]. For $\gamma^q = 0$, the spin length is fixed and ψ is redundant, recovering the usual Bloch-sphere description. More generally, ψ is required to capture spin-length mixing under local dissipation. As it is absent in Weyl symbols of collective observables, it serves here as an auxiliary variable in practice [57].

With the quantum-classical mapping specified, we take the semiclassical limit of Eq. (1). For large spin lengths, treating $\mathcal{J} \gg 1$ as continuous yields the semiclassical expansion [51, 54],

$$\text{Tr} [\hat{O} \hat{O}' \hat{\Delta}] \approx \mathcal{O} \mathcal{O}' + \frac{i}{2} \{\mathcal{O}, \mathcal{O}'\}, \quad (5)$$

up to relative corrections $O(\mathcal{J}^{-1})$, which are typically of order N^{-1} . The Poisson bracket $\{\bullet, \bullet\}$ corresponds to a symmetric top on the *four-dimensional* phase space $\mathcal{Z} = (\phi, \theta, \psi, \mathcal{J})$, where the conjugate variable ψ now captures fluctuations in spin length [37]. Substituting Eq. (5) into Eq. (1) yields a truncated-Wigner Fokker-Planck equation for W with positive-semidefinite diffusion [58, 59], which can be equivalently unraveled into Stratonovich stochastic differential (Langevin) equations:

$$\frac{d\mathcal{Z}}{dt} = \{\mathcal{Z}, \mathcal{H}\} + \text{Re} \left[\sum_k \{\mathcal{Z}, \sqrt{r_k} \mathcal{L}_k\} \circ (\eta_k + i\sqrt{r_k} \mathcal{L}_k^*) \right]. \quad (6)$$

Here η_k are independent complex white noise processes, $\langle \eta_k(t) \eta_{k'}^*(t') \rangle / 2 = \delta_{kk'} \delta(t - t')$, with \circ denoting Stratonovich multiplication. $\{\mathcal{L}_k, r_k\}$ are the Weyl symbols and corresponding rates of jump operators, $\mathcal{L}_k = \ell^{jq}, \mathcal{L}^q, r_k = \gamma^q, \Gamma^q$, for the dissipation channel index k .

To finally estimate expectations in the TWA, we average the Weyl symbols over the N_{traj} trajectories $\mathcal{Z}^{(i)}(t)$ that sample W at time t ,

$$\langle \hat{O}(t) \rangle \approx \frac{1}{N_{\text{traj}}} \sum_{i=1}^{N_{\text{traj}}} \mathcal{O}(\mathcal{Z}^{(i)}(t)), \quad (7)$$

with phase-space variables initialized from the Wigner function of a fully-polarized state [53] and evolved using Eq. (6). In the following, $N_{\text{traj}} = 10^3\text{--}10^6$ typically renders sampling errors of order $1/\sqrt{N_{\text{traj}}}$ negligible, with

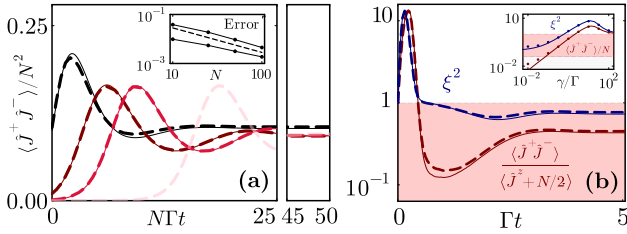


Fig. 2. Dynamics of an emitter ensemble under local pumping and collective decay. (a) Evolution of normalized emission rate $\langle \hat{J}^+ \hat{J}^- \rangle / N^2$ for $N = 10, 10^2, 10^3$, and 10^6 (dark to light), for scaled time NTt . Solid curves show exact results, with TWA shown as dashed curves. For $N = 10^6$, exact simulation is not feasible here. Inset: maximum error between TWA and exact dynamics for the normalized emission rate (lower line) and normalized inversion $\langle \hat{J}^z \rangle / N$ (upper line), compared to a $1/N$ reference (dashed). (b) Squeezing parameter ξ^2 and subradiance parameter $s = \langle \hat{J}^+ \hat{J}^- \rangle / (\langle \hat{J}^z \rangle + N/2)$ for $N = 25$. Inset: steady-state emission rate $\langle \hat{J}^+ \hat{J}^- \rangle / N$ versus pump rate for TWA (dots) and exact solution (solid line); red shaded region indicates values less than one, and the gray region marks the threshold of TWA validity where $\langle \hat{J}^+ \hat{J}^- \rangle$ is of order one.

errors reduced for larger N . By evolving only four phase-space variables in parallel per ensemble, this method enables simulation of dynamics in systems from a few emitters to the limit of large ensemble size.

We have numerically verified the accuracy of this general TWA in a number of systems, including boundary time crystals subject to decoherence, and standard superradiant decay [53]. To illustrate the key aspects, we focus here on emission dynamics in the model of a bad-cavity superradiant laser [1, 15], in which collective decay Γ (for $q = -1$) competes with incoherent individual pumping γ ($q = 1$), and $\hat{H} = 0$. These dynamics admit exact Monte Carlo simulations [60], allowing us to verify our results for up to tens of thousands of atoms. While we present two-body observables capturing output emission, we have found that single-body expectations, such as ensemble inversion, are generally predicted with similar accuracy [53].

In Fig. 2(a), we calculate the evolution of normalized intensity $\langle \hat{J}^+ \hat{J}^- \rangle / N^2$ for a fully-inverted ensemble as N is increased from ten up to one million. The pump $\gamma = 0.25NT$ is chosen to maintain competition with decay. For ensembles as small as $N = 10$, our method accurately captures, with less than 10% deviation, the transient superradiant pulse, subsequent relaxations, and the collective steady-state emission. Crucially, the accuracy increases with N . Already for $N \simeq 100$ our predictions agree closely with exact dynamics, and we have quantitatively verified that the prediction error of the TWA decreases with increasing emitter number [Fig. 2(a), inset]. This is consistent with the perturbative expansion Eq. (5), as \mathcal{J} is typically of the order N in individual trajectories. These benchmarks establish the TWA as a

reliable semiclassical method for approximating the dynamics of permutation-invariant emitter ensembles.

To demonstrate how the TWA captures nonclassical dynamics, Fig. 2(b) presents the generalized squeezing parameter [61] $\xi^2 = \langle (\Delta \hat{J}^x)^2 + (\Delta \hat{J}^y)^2 + (\Delta \hat{J}^z)^2 \rangle / (N/2)$ for a weak pump $\gamma = 0.4\Gamma$ and moderate $N = 25$. A value $\xi^2 < 1$ indicates entanglement relevant for quantum information [62]. The TWA closely reproduces both the transient reduction below unity and the subsequent relaxation to the steady-state. Beyond squeezing, the TWA can also capture subradiance—absent at mean-field level for homogeneous ensembles—where destructive interference suppresses the normalized collective emission rate, $s = \langle \hat{J}^+ \hat{J}^- \rangle / (\langle \hat{J}^z \rangle + N/2)$, below that of independent emitters ($s = 1$), offering a distinct resource for metrology [17, 63]. In Fig. 2(b), the TWA accurately predicts the evolution towards $s < 1$ and confirms subradiance as a precursor to squeezing in this system [64]. Noticeable deviations from the exact dynamics are confined to the extremely subradiant regime $\langle \hat{J}^+ \hat{J}^- \rangle \lesssim 1$, which coincides with a reduction $\mathcal{J} \sim O(1)$ along individual trajectories—signaling the importance of higher-order terms beyond Eq. (5) and providing a practical diagnostic of accuracy. Away from this regime, the inset of Fig. 2(b) shows that TWA can remain quantitatively accurate across a broad parameter range.

The TWA extends naturally from a single ensemble to composite systems that partition into distinct homogeneous ensembles, including waveguide-coupled emitter arrays, inhomogeneously broadened ensembles, and ensembles in extended resonator lattices [Fig. 3(a)]. By assigning independent phase-space variables \mathcal{Z}_ℓ to each ensemble and evolving Eq. (6), quantum dynamics can be captured with a computational cost that scales linearly with the number of distinct ensembles. As an example, we consider an infinite 1D lattice of coupled resonators in which a subset of M equally spaced sites each hosts a resonant ensemble containing N emitters, for a total $N_{\text{tot}} = NM$. In the bad-cavity limit, adiabatic elimination of the photonic degrees of freedom yields an effective master equation for the collective spins, with resonator-mediated coherent couplings and dissipative jumps:

$$\hat{H} = \frac{\Gamma}{2} \sum_{\ell, \ell'=1}^M \sin(\varphi|\ell - \ell'|) \hat{J}_\ell^+ \hat{J}_{\ell'}^-, \quad \hat{L}_{\text{F(B)}} = \sum_{\ell=1}^M e^{\pm i\varphi\ell} \hat{J}_\ell^-. \quad (8)$$

In this model, Γ denotes the single-emitter decay rate into the chain and φ is the phase accumulated between neighboring populated sites. The jump operators \hat{L}_{F} and \hat{L}_{B} describe collective emission into forward and backward propagating modes, each at rate $\Gamma/2$. This setup realizes the waveguide-QED paradigm [65] where ensembles act as super-atoms, offering a broad landscape of collective dynamics in the TWA.

Using the model Eq. (8), we assess the TWA in a composite system where inter-ensemble coupling com-

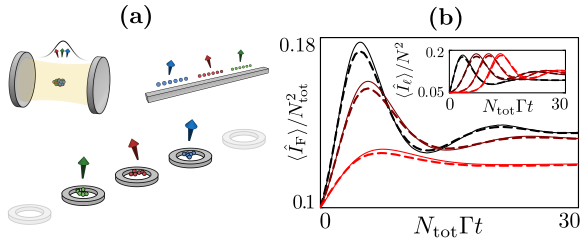


Fig. 3. (a) Illustration of composite systems described using the TWA by assigning a collective spin to each permutation-invariant constituent (indicated by color). (b) Forward emission rate $\langle \hat{I}_F \rangle / N_{\text{tot}}^2$ for $M = 2$ pumped ensembles, each comprising $N = 20$ emitters for a total $N_{\text{tot}} = 40$. The propagation phase $\varphi = 0, \pi/4, \pi/2$ (upper to lower curves). Emitters are initially in the ground state, and the local pump $\gamma = 10\Gamma$. Inset: (identical) single-ensemble emission rates $\langle \hat{I}_\ell \rangle / N^2$ for $\varphi = 0$ as the number of ensembles is increased with $M = 1, 10, 10^2, 10^3$ (dark to light) and $\gamma = 0.25N_{\text{tot}}\Gamma$. Solid (dashed) curves give the exact solution (TWA).

petes with local pumping. Already for $M = 2$, this model supports synchronization and rapid energy transport [13, 66], but more generally, the propagation phase φ can suppress cooperativity and its impact on pumped ensembles has been less explored. Comparing with exact simulations for $N = 20$, we compute the forward emission $\langle \hat{I}_F \rangle = \langle \hat{L}_F^\dagger \hat{L}_F \rangle$ and find a pronounced reduction in the transient superradiant peak with increasing φ , accurately captured by the TWA. At $\varphi = \pi/2$, the steady-state emission is suppressed by nearly 50% [Fig. 3(b)], highlighting the impact of phase-dependent coherent coupling in extended 1D geometries. Despite the additional coherent terms, the level of agreement between the TWA and exact solutions remains comparable to the single-ensemble case.

To assess the TWA in larger systems, we compare with exact Monte Carlo evolution in the limit $\varphi = 0$, where simulations remain feasible for large arrays, and find that the TWA also tracks site-resolved emission $\langle \hat{I}_\ell \rangle = \langle \hat{J}_\ell^+ \hat{J}_\ell^- \rangle$ for up to one thousand ensembles. As observed previously, the agreement improves with emitter number N , giving qualitative accuracy for $N \simeq 10$ and close quantitative agreement for $N \gtrsim 100$.

The scalability of the TWA enables simulations of dynamics rooted in microscopic models in regimes that can be challenging to reliably access with established methods. In Fig. 4, we present TWA simulations of large-scale dynamics in an extended nonlinear medium formed from a chain of $M = 100$ ensembles ($N = 250$) under uniform pumping $\gamma = 250\Gamma$, with incommensurate phase $\varphi = \pi/10$. Here, we have confirmed that the control parameter \mathcal{J}^{-1} generally remains comparable to N^{-1} in individual trajectories. Following an initial synchronized superradiant burst, the total forward emission reaches its steady value within a time $t \simeq 0.01 \times 1/\Gamma$. However, on the longer timescale $t \simeq 1/\Gamma$, the emission redis-

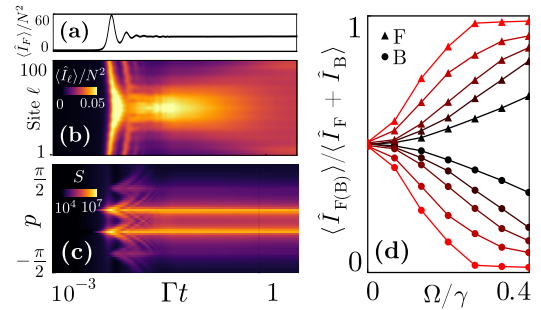


Fig. 4. Emission dynamics in a 1D chain of M ensembles, for emitters initially in the ground state. (a) Normalized total forward emission rate $\langle \hat{I}_F \rangle / N^2$, (b) local emission rate $\langle \hat{I}_\ell \rangle / N^2$, and (c) spatial structure factor $S(p)$ as a function of time (log-axis). (d) Forward and backward intensity fractions versus normalized drive strength Ω/γ with $M = 20, 30, 50, 100$, and 500 (dark to light), fixing accumulated phase $M\varphi = 10\pi$ and effective cooperativity $\Gamma N_{\text{tot}}/\gamma = 100$.

tributes across the chain and relaxes—despite uniform pumping—to a steady state with a weakly modulated profile. Calculating the unnormalized structure factor $S(p) = \sum_{k,\ell} e^{ip(k-\ell)} \langle \hat{J}_k^+ \hat{J}_\ell^- \rangle$ for dimensionless momentum p in Fig. 4(c), the development of two sharp emergent peaks in the spectrum indicates spatial coherence of emission in the populations of symmetric, oppositely propagating waves.

Excitation of counter-propagating waves under pumping is consistent with emergent directionality of emission in ring geometries of bulk nonlinear media [67, 68] and microscopic atomic arrays [69]. We then probe the susceptibility to a weak, resonant forward-propagating coherent field, $\hat{H}_{\text{drv}} = \Omega \sum_\ell (e^{i\varphi\ell} \hat{J}_\ell^+ + \text{h.c.})$, to break the mirror symmetry in systems of up to $M = 500$, evaluating the forward and backward intensities at late times $t = 2/\Gamma$. Fig. 4(d) shows the resulting asymmetry as a function of drive with M increasing from 20 to 500, keeping the medium phase $M\varphi$ and effective cooperativity $\Gamma M N / \gamma$ fixed. The fraction of intensity in the forward mode increases with the drive, exhibiting a response that steepens systematically with increasing M . The largest system, $M = 500$, displays a pronounced saturation towards unidirectional emission, indicating a strong and size-dependent directional response in extended 1D media, accessible within the TWA.

Our results establish a semiclassical framework for large, permutation-invariant ensembles subject to dissipation, bridging microscopic master equations to large-scale collective effects. By leveraging a symmetry-adapted phase space, the approach naturally incorporates system structure, with possible extensions to include (ultra)strong coupling to bosonic modes [20, 70], internal level structure [57, 71, 72], and non-Markovian dynamics [73, 74].

As experiments in cavity [7, 59, 75–77] and waveg-

uide QED [78] enter the mesoscopic regime, realizing extended architectures with multiple interacting ensembles [79–82], our work provides a compact ensemble-level phase-space description to complement existing numerical methods. Rooted in a perturbative semiclassical limit, our approach can help elucidate how realistic dissipation reshapes emergent behaviors such as synchronization [10, 13, 83, 84] and time-crystalline dynamics [10, 83], providing essential guidance for emerging quantum technologies [77, 85–88] powered by cooperative phenomena.

We acknowledge financial support, in part, from Moonshot R&D, JST JPMJMS2061. We appreciate discussions with William J. Munro and Victor M. Bastidas.

[1] J. G. Bohnet, Z. Chen, J. M. Weiner, D. Meiser, M. J. Holland, and J. K. Thompson, A steady-state superradiant laser with less than one intracavity photon, *Nature* **484**, 78 (2012).

[2] K. Baumann, C. Guerlin, F. Brennecke, and T. Esslinger, Dicke quantum phase transition with a superfluid gas in an optical cavity, *Nature* **464**, 1301 (2010).

[3] P. F. Herskind, A. Dantan, J. P. Marler, M. Albert, and M. Drewsen, Realization of collective strong coupling with ion Coulomb crystals in an optical cavity, *Nature Physics* **5**, 494 (2009).

[4] M. Gärttner, J. G. Bohnet, A. Safavi-Naini, M. L. Wall, J. J. Bollinger, and A. M. Rey, Measuring out-of-time-order correlations and multiple quantum spectra in a trapped-ion quantum magnet, *Nature Physics* **13**, 781 (2017).

[5] M. Scheibner, T. Schmidt, L. Worschech, A. Forchel, G. Bacher, T. Passow, and D. Hommel, Superradiance of quantum dots, *Nature Phys.* **3**, 106 (2007).

[6] X. Zhu, S. Saito, A. Kemp, K. Kakuyanagi, S.-i. Karmoto, H. Nakano, W. J. Munro, Y. Tokura, M. S. Everitt, K. Nemoto, M. Kasu, N. Mizuuchi, and K. Semba, Coherent coupling of a superconducting flux qubit to an electron spin ensemble in diamond, *Nature* **478**, 221 (2011).

[7] M. Lei, R. Fukumori, J. Rochman, B. Zhu, M. Endres, J. Choi, and A. Faraon, Many-body cavity quantum electrodynamics with driven inhomogeneous emitters, *Nature* **617**, 271 (2023).

[8] J. Q. Quach, K. E. McGhee, L. Ganzer, D. M. Rouse, B. W. Lovett, E. M. Gauger, J. Keeling, G. Cerullo, D. G. Lidzey, and T. Virgili, Superabsorption in an organic microcavity: Toward a quantum battery, *Science Advances* **8**, eabk3160 (2022).

[9] K. Kakuyanagi, Y. Matsuzaki, C. Déprez, H. Toida, K. Semba, H. Yamaguchi, W. J. Munro, and S. Saito, Observation of collective coupling between an engineered ensemble of macroscopic artificial atoms and a superconducting resonator, *Phys. Rev. Lett.* **117**, 210503 (2016).

[10] Z. Wang, R. Gao, X. Wu, B. Buća, K. Mølmer, L. You, and F. Yang, Boundary time crystals induced by local dissipation and long-range interactions, *Phys. Rev. Lett.* **135**, 230401 (2025).

[11] P. Kirton and J. Keeling, Suppressing and restoring the dicke superradiance transition by dephasing and decay, *Phys. Rev. Lett.* **118**, 123602 (2017).

[12] T. E. Lee, C.-K. Chan, and S. F. Yelin, Dissipative phase transitions: Independent versus collective decay and spin squeezing, *Phys. Rev. A* **90**, 052109 (2014).

[13] M. Xu, D. A. Tieri, E. C. Fine, J. K. Thompson, and M. J. Holland, Synchronization of two ensembles of atoms, *Phys. Rev. Lett.* **113**, 154101 (2014).

[14] T. E. Lee, H. Häffner, and M. C. Cross, Collective quantum jumps of Rydberg atoms, *Phys. Rev. Lett.* **108**, 023602 (2012).

[15] D. Meiser, J. Ye, D. R. Carlson, and M. J. Holland, Prospects for a millihertz-linewidth laser, *Phys. Rev. Lett.* **102**, 163601 (2009).

[16] F. Reiter, D. Reeb, and A. S. Sørensen, Scalable dissipative preparation of many-body entanglement, *Phys. Rev. Lett.* **117**, 040501 (2016).

[17] L. Ostermann, H. Ritsch, and C. Genes, Protected state enhanced quantum metrology with interacting two-level ensembles, *Phys. Rev. Lett.* **111**, 123601 (2013).

[18] K. Tucker, D. Barberena, R. J. Lewis-Swan, J. K. Thompson, J. G. Restrepo, and A. M. Rey, Facilitating spin squeezing generated by collective dynamics with single-particle decoherence, *Phys. Rev. A* **102**, 051701 (2020).

[19] B. A. Chase and J. M. Geremia, Collective processes of an ensemble of spin-1/2 particles, *Phys. Rev. A* **78**, 052101 (2008).

[20] N. Shammah, S. Ahmed, N. Lambert, S. De Liberato, and F. Nori, Open quantum systems with local and collective incoherent processes: Efficient numerical simulations using permutational invariance, *Phys. Rev. A* **98**, 063815 (2018).

[21] S. Sarkar and J. S. Satchell, Solution of master equations for small bistable systems, *J. Phys. A* **20**, 2147 (1987).

[22] M. Xu, D. A. Tieri, and M. J. Holland, Simulating open quantum systems by applying SU(4) to quantum master equations, *Phys. Rev. A* **87**, 062101 (2013).

[23] P. Kirton and J. Keeling, Suppressing and restoring the dicke superradiance transition by dephasing and decay, *Phys. Rev. Lett.* **118**, 123602 (2017).

[24] M. Gegg and M. Richter, PsiQuaSP—A library for efficient computation of symmetric open quantum systems, *Scientific Reports* **7**, 16304 (2017).

[25] H. Weimer, A. Kshetrimayum, and R. Orús, Simulation methods for open quantum many-body systems, *Rev. Mod. Phys.* **93**, 015008 (2021).

[26] R. Kubo, Generalized cumulant expansion method, *Journal of the Physical Society of Japan* **17**, 1100 (1962).

[27] D. Plankensteiner, C. Hotter, and H. Ritsch, Quantum-cumulants. jl: A Julia framework for generalized mean-field equations in open quantum systems, *Quantum* **6**, 617 (2022).

[28] F. Verstraete, J. J. García-Ripoll, and J. I. Cirac, Matrix product density operators: Simulation of finite-temperature and dissipative systems, *Phys. Rev. Lett.* **93**, 207204 (2004).

[29] M. Zwolak and G. Vidal, Mixed-state dynamics in one-dimensional quantum lattice systems: A time-dependent superoperator renormalization algorithm, *Phys. Rev. Lett.* **93**, 207205 (2004).

[30] J. Schachenmayer, A. Pikovski, and A. M. Rey, Many-body quantum spin dynamics with monte carlo trajectories on a discrete phase space, *Phys. Rev. X* **5**, 011022

(2015).

[31] C. D. Mink, D. Petrosyan, and M. Fleischhauer, Hybrid discrete-continuous truncated Wigner approximation for driven, dissipative spin systems, *Phys. Rev. Res.* **4**, 043136 (2022).

[32] V. P. Singh and H. Weimer, Driven-dissipative criticality within the Discrete Truncated Wigner Approximation, *Phys. Rev. Lett.* **128**, 200602 (2022).

[33] J. Huber, A. M. Rey, and P. Rabl, Realistic simulations of spin squeezing and cooperative coupling effects in large ensembles of interacting two-level systems, *Phys. Rev. A* **105**, 013716 (2022).

[34] H. Hosseinabadi, O. Chelpanova, and J. Marino, User-friendly Truncated Wigner Approximation for dissipative spin dynamics, *PRX Quantum* **6**, 030344 (2025).

[35] K. Merkel, V. Link, K. Luoma, and W. T. Strunz, Phase space theory for open quantum systems with local and collective dissipative processes, *Journal of Physics A: Mathematical and Theoretical* **54**, 035303 (2020).

[36] A. Kolmer Forbes, P. Daniel Blocher, and I. H. Deutsch, Modeling local decoherence of a spin ensemble using a generalized Holstein-Primakoff mapping to a bosonic mode, *Optica Quantum* **2**, 310 (2024).

[37] D. Barberena, Generalized Holstein-Primakoff mapping and $1/N$ expansion of collective spin systems undergoing single particle dissipation, *arXiv preprint arXiv:2508.05751* (2025).

[38] J. E. Moyal, Quantum mechanics as a statistical theory, in *Mathematical Proceedings of the Cambridge Philosophical Society*, Vol. 45 (Cambridge University Press, 1949) pp. 99–124.

[39] R. P. Rundle and M. J. Everitt, Overview of the phase space formulation of quantum mechanics with application to quantum technologies, *Advanced Quantum Technologies* **4**, 2100016 (2021).

[40] D. F. Walls and G. J. Milburn, *Quantum Optics* (Springer, Berlin and New York, 1994).

[41] A. Polkovnikov, Phase space representation of quantum dynamics, *Annals of Physics* **325**, 1790 (2010).

[42] M. J. Steel, M. K. Olsen, L. I. Plimak, P. D. Drummond, S. M. Tan, M. J. Collett, D. F. Walls, and R. Graham, Dynamical quantum noise in trapped Bose-Einstein condensates, *Phys. Rev. A* **58**, 4824 (1998).

[43] P. Filipowicz, J. Javanainen, and P. Meystre, Quantum and semiclassical steady states of a kicked cavity mode, *Journal of the Optical Society of America B* **3**, 906 (1986).

[44] F. Vicentini, F. Minganti, R. Rota, G. Orso, and C. Ciuti, Critical slowing down in driven-dissipative Bose-Hubbard lattices, *Phys. Rev. A* **97**, 013853 (2018).

[45] P. Blakie, A. Bradley, M. Davis, R. Ballagh, and C. Gardiner, Dynamics and statistical mechanics of ultra-cold bose gases using c-field techniques, *Advances in Physics* **57**, 363 (2008).

[46] F. Haake, M. Kuš, and R. Scharf, Classical and quantum chaos for a kicked top, *Zeitschrift für Physik B Condensed Matter* **65**, 381 (1987).

[47] J. C. Várilly and J. Gracia-Bondía, The Moyal representation for spin, *Annals of physics* **190**, 107 (1989).

[48] J. Huber, P. Kirton, and P. Rabl, Phase-space methods for simulating the dissipative many-body dynamics of collective spin systems, *SciPost Physics* **10**, 045 (2021).

[49] A. Altland, V. Gurarie, T. Kricheverbauer, and A. Polkovnikov, Nonadiabaticity and large fluctuations in a many-particle Landau-Zener problem, *Phys. Rev. A* **79**, 042703 (2009).

[50] A. B. Klimov, J. L. Romero, and H. de Guise, Generalized SU(2) covariant Wigner functions and some of their applications, *Journal of Physics A: Mathematical and Theoretical* **50**, 323001 (2017).

[51] A. B. Klimov and J. Romero, A generalized wigner function for quantum systems with the SU(2) dynamical symmetry group, *Journal of Physics A: Mathematical and Theoretical* **41**, 055303 (2008).

[52] B. Q. Baragiola, B. A. Chase, and J. Geremia, Collective uncertainty in partially polarized and partially decohered spin-1 systems, *Phys. Rev. A* **81**, 032104 (2010).

[53] See supplemental material for additional details regarding technical background information.

[54] K. Tomatani, J. L. Romero, and A. B. Klimov, Semiclassical phase-space dynamics of compound quantum systems: SU(2) covariant approach, *Journal of Physics A: Mathematical and Theoretical* **48**, 215303 (2015).

[55] T. Tilma, M. J. Everitt, J. H. Samson, W. J. Munro, and K. Nemoto, Wigner functions for arbitrary quantum systems, *Phys. Rev. Lett.* **117**, 180401 (2016).

[56] C. Brif and A. Mann, Phase-space formulation of quantum mechanics and quantum-state reconstruction for physical systems with lie-group symmetries, *Phys. Rev. A* **59**, 971 (1999).

[57] S. M. Davidson and A. Polkovnikov, SU(3) semiclassical representation of quantum dynamics of interacting spins, *Phys. Rev. Lett.* **114**, 045701 (2015).

[58] J. Dubois, U. Saalmann, and J. M. Rost, Semi-classical Lindblad master equation for spin dynamics, *Journal of Physics A: Mathematical and Theoretical* **54**, 235201 (2021).

[59] A. Periwal, E. S. Cooper, P. Kunkel, J. F. Wienand, E. J. Davis, and M. Schleier-Smith, Programmable interactions and emergent geometry in an array of atom clouds, *Nature* **600**, 630 (2021).

[60] Y. Zhang, Y.-X. Zhang, and K. Mølmer, Monte-Carlo simulations of superradiant lasing, *New Journal of Physics* **20**, 112001 (2018).

[61] G. Tóth, C. Knapp, O. Gühne, and H. J. Briegel, Optimal spin squeezing inequalities detect bound entanglement in spin models, *Phys. Rev. Lett.* **99**, 250405 (2007).

[62] J. Ma, X. Wang, C. Sun, and F. Nori, Quantum spin squeezing, *Physics Reports* **509**, 89 (2011).

[63] G. Facchinetto, S. D. Jenkins, and J. Ruostekoski, Storing light with subradiant correlations in arrays of atoms, *Phys. Rev. Lett.* **117**, 243601 (2016).

[64] A. Shankar, J. T. Reilly, S. B. Jäger, and M. J. Holland, Subradiant-to-subradiant phase transition in the bad cavity laser, *Phys. Rev. Lett.* **127**, 073603 (2021).

[65] A. S. Sheremet, M. I. Petrov, I. V. Iorsh, A. V. Poshakinskiy, and A. N. Poddubny, Waveguide quantum electrodynamics: Collective radiance and photon-photon correlations, *Rev. Mod. Phys.* **95**, 015002 (2023).

[66] M. Fässer, L. Ostermann, H. Ritsch, and C. Hotter, Subradiance and superradiant long-range excitation transport among quantum emitter ensembles in a waveguide, *Optica Quantum* **2**, 397 (2024).

[67] A. E. Kaplan and P. Meystre, Enhancement of the sagnac effect due to nonlinearly induced nonreciprocity, *Opt. Lett.* **6**, 590 (1981).

[68] L. Del Bino, J. M. Silver, S. L. Stebbings, and P. Del'Haye, Symmetry Breaking of Counter-

Propagating Light in a Nonlinear Resonator, *Scientific Reports* **7**, 43142 (2017).

[69] S. Cardenas-Lopez, E. Guardiola-Navarrete, and A. Asenjo-Garcia, Emergent spin order and steady-state superradiance in one-dimensional baths, *arXiv preprint arXiv:2511.10638* (2025).

[70] E. K. Twyeffort Irish and A. D. Armour, Defining the semiclassical limit of the Quantum Rabi hamiltonian, *Phys. Rev. Lett.* **129**, 183603 (2022).

[71] M. Gegg and M. Richter, Efficient and exact numerical approach for many multi-level systems in open system qed, *New Journal of Physics* **18**, 043037 (2016).

[72] B. Zhu, A. M. Rey, and J. Schachenmayer, A generalized phase space approach for solving quantum spin dynamics, *New Journal of Physics* **21**, 082001 (2019).

[73] H. Pichler and P. Zoller, Photonic circuits with time delays and quantum feedback, *Phys. Rev. Lett.* **116**, 093601 (2016).

[74] B. Windt, M. Bello, D. Malz, and J. I. Cirac, Effects of retardation on many-body superradiance in chiral waveguide QED, *Phys. Rev. Lett.* **134**, 173601 (2025).

[75] V. D. Vaidya, Y. Guo, R. M. Kroese, K. E. Ballantine, A. J. Kollár, J. Keeling, and B. L. Lev, Tunable-range, photon-mediated atomic interactions in multimode cavity qed, *Phys. Rev. X* **8**, 011002 (2018).

[76] T. Astner, S. Nevlacsil, N. Peterschofsky, A. Angerer, S. Rotter, S. Putz, J. Schmiedmayer, and J. Majer, Coherent coupling of remote spin ensembles via a cavity bus, *Phys. Rev. Lett.* **118**, 140502 (2017).

[77] J. M. Robinson, M. Miklos, Y. M. Tso, C. J. Kennedy, T. Bothwell, D. Kedar, J. K. Thompson, and J. Ye, Direct comparison of two spin-squeezed optical clock ensembles at the 10^{-17} level, *Nature Physics* **20**, 208 (2024).

[78] C. Liedl, F. Tebbenjohanns, C. Bach, S. Pucher, A. Rauschenbeutel, and P. Schneeweiss, Observation of superradiant bursts in a cascaded quantum system, *Phys. Rev. X* **14**, 011020 (2024).

[79] S. Kato, N. Német, K. Senga, S. Mizukami, X. Huang, S. Parkins, and T. Aoki, Observation of dressed states of distant atoms with delocalized photons in coupled-cavities quantum electrodynamics, *Nature Communications* **10**, 1160 (2019).

[80] Y. Yu, F. Ma, X.-Y. Luo, B. Jing, P.-F. Sun, R.-Z. Fang, C.-W. Yang, H. Liu, M.-Y. Zheng, X.-P. Xie, W.-J. Zhang, L.-X. You, Z. Wang, T.-Y. Chen, Q. Zhang, X.-H. Bao, and J.-W. Pan, Entanglement of two quantum memories via fibres over dozens of kilometres, *Nature* **578**, 240 (2020).

[81] C.-X. Run, K.-T. Lin, K.-M. Hsieh, B.-Y. Wu, W.-M. Zhou, G.-D. Lin, A. Kockum, and I.-C. Hoi, Realizing on-demand all-to-all selective interactions between distant spin ensembles, *arXiv preprint arXiv:2512.07326* (2025).

[82] L. J. Zou, D. Marcos, S. Diehl, S. Putz, J. Schmiedmayer, J. Majer, and P. Rabl, Implementation of the Dicke lattice model in hybrid quantum system arrays, *Phys. Rev. Lett.* **113**, 023603 (2014).

[83] P. Solanki, M. Krishna, M. Hajdušek, C. Bruder, and S. Vinjanampathy, Exotic synchronization in continuous time crystals outside the symmetric subspace, *Phys. Rev. Lett.* **133**, 260403 (2024).

[84] T. Nadolny, C. Bruder, and M. Brunelli, Nonreciprocal synchronization of active quantum spins, *Phys. Rev. X* **15**, 011010 (2025).

[85] J. R. K. Cline, V. M. Schäfer, Z. Niu, D. J. Young, T. H. Yoon, and J. K. Thompson, Continuous collective strong coupling of strontium atoms to a high finesse ring cavity, *Phys. Rev. Lett.* **134**, 013403 (2025).

[86] W. Niedenzu and G. Kurizki, Cooperative many-body enhancement of quantum thermal machine power, *New Journal of Physics* **20**, 113038 (2018).

[87] V. Montenegro, M. G. Genoni, A. Bayat, and M. G. A. Paris, Quantum metrology with boundary time crystals, *Communications Physics* **6**, 304 (2023).

[88] K. Hymas, J. B. Muir, D. Tibben, J. van Embden, T. Hirai, C. J. Dunn, D. E. Gómez, J. A. Hutchison, T. A. Smith, and J. Q. Quach, Experimental demonstration of a scalable room-temperature quantum battery, *arXiv preprint arXiv:2501.16541* (2025).